Scanning Electron Microscopy

Volume 1986 | Number 2 Article 5

7-10-1986

Charging Effects in Low-Voltage Scanning Electron Microscope Metrology

M. Brunner
Research Laboratories of Siemens AG

R. Schmid
Universität Tübingen

Follow this and additional works at: https://digitalcommons.usu.edu/electron

Part of the Biology Commons

Recommended Citation

Brunner, M. and Schmid, R. (1986) "Charging Effects in Low-Voltage Scanning Electron Microscope Metrology," *Scanning Electron Microscopy*: Vol. 1986 : No. 2 , Article 5.
Available at: https://digitalcommons.usu.edu/electron/vol1986/iss2/5

This Article is brought to you for free and open access by the Western Dairy Center at DigitalCommons@USU. It has been accepted for inclusion in Scanning Electron Microscopy by an authorized administrator of DigitalCommons@USU. For more information, please contact digitalcommons@usu.edu.

SCANNING ELECTRON MICROSCOPY/1986/II (Pages 377-382)
SEM Inc., AMF O'Hare (Chicago), IL 60666-0507 USA
0586-5581/86$1.00+05

CHARGING EFFECTS IN LOW-VOLTAGE SCANNING ELECTRON MICROSCOPE METROLOGY

M. Brunner* and R. Schmid**

* Research Laboratories of Siemens AG, München, Germany
** Institut für Angewandte Physik, Universität Tübingen, Germany

(Received for publication March 13, 1986: revised paper received July 10, 1986)

Abstract

Low voltage operation of the scanning electron microscope is being increasingly used to avoid negative charging in e-beam inspection and metrology. Positive charging effects, however, may still disturb the measurement accuracy even with low primary beam energies. Current investigations have revealed that no errors due to positive charging occur on resist structures on semiconductor substrates. But samples with metal structures on insulating substrates do involve disturbing effects due to positive charging. The difference in behavior between these groups of samples is attributed to the fundamental difference between insulator and conductor charging. This difference is due to different field geometries on the respective surfaces.

Key Words: Scanning electron microscope, integrated circuit, mask, inspection, metrology, charging, low-voltage.

*Address for correspondence: M. Brunner
Research Laboratories of Siemens AG
Otto-Hahn Ring 6, D-8000 München 83
W. Germany Phone no.: (089) 636-44175

Introduction

New methods of inspection and metrology are required in manufacturing integrated circuits and components for optical communications, since structures are approaching dimensions below 1 µm. Light-optical methods are reaching their limit of resolution at this stage of miniaturization. Scanning electron microscopes (SEMs) are therefore being increasingly employed for dimensional and quality control in the manufacturing processes (Postek 1983,1984a,b; Frosien and Lischke 1984;Frosien 1986; Russel et al. 1984; Yamaji et al. 1985).In general, the line width and pitch of structures on integrated circuits or masks are the quantities to be measured. Several SEM manufacturers already offer dedicated machines with a high degree of automation and computer-assisted pattern evaluation.

The success of SEM applications depends on the accuracy and reliability of the method and the instrument. Limitations to the SEM measurement accuracy are caused by 1) the instrument and by 2) beam-sample interactions. Instrument related limitations have been discussed in several papers (Jensen & Swyt 1980, Seiler & Sulway 1984; Russel et al. 1984) while effects of beam sample interactions have not yet been fully investigated. The impact of electron scattering and secondary electron generation on the problem of locating the actual feature edge from the acquired secondary electron intensity profile is frequently considered (Jensen et al. 1981; Hembree et al. 1981, Russel et al. 1984, Nyyssonen and Postek 1985; Yamaji et al. 1985). Little attention has been paid to charging effects which can influence the intensity profile (Yamaji et al. 1985) and which can also displace the beam. One of the main requirements of SEM applicability is the avoidance of charging effects without sample surface coating. Inspected devices, e.g. resist structures, can then continue to be processed. Specimen charging is avoided by the basic idea of compensating the primary beam current I_P by the emitted currents of secondary I_S and backscattered I_B electrons. Balance between impinging and emitted currents appears at a certain energy E_N (Fig. 1) of the incident electrons, which is in the range of 1 keV or below (e.g. Gibbons 1966; Brunner and Menzel 1983). The second crossover at

lower energy is not considered here because it does not allow stable, non-charging operation.

The energy E_N depends on several parameters, such as surface material, surface roughness and surface angle (Fig. 1). This is why complex structures containing several materials with different surface conditions and angles will generally not allow balancing of emitted and incident currents on the whole sample simultaneously. Consider a beam energy E being adjusted to a point above the values E_N' of certain surface areas charging these areas to negative potentials because the number of incident electrons exceeds the number of emitted electrons. Other areas having higher values $E_N'' > E$ will then charge positively with the same primary beam energy E, since the number of incident electrons is less than the number of emitted electrons. Even if the primary energy E is chosen to be smaller than E_N on all surface areas, positive charging will not, in general, result in a uniform surface voltage. The nature of these remaining charging effects and their influence on image distortions and measurement accuracy are the subject of current investigations. This paper focuses on beam displacement and related distortions and does not discuss the specific contrast effects in the low-voltage SEM which are partly also due to surface charging.

Nature of charging effects in low-voltage SEMs

While negative charging in high-voltage SEMs has been studied in detail by Crawford (1980), the positive charging effects associated with low-voltage electron beams have not. The aim is therefore to develop an initial theoretical statement about positive specimen charging.

Consider a planar surface of an insulator or floating conductor being bombarded with electrons of energy $E < E_N$ (Fig. 1). The electrons are focused to form a small spot which scans the surface in a raster. Secondary electrons are emitted from the surface element, irradiated by the primary spot and attracted by the collecting grid of the detector. In this picture, the scanning of the primary beam is described by a dwell time t_i on each irradiated surface element i and a subsequent jump to the adjacent one. After frame time T, the first element is addressed again. The element is assumed to have a capacitance C to ground, which charges positively during the dwell time t_i since $E < E_N$ and due to the extraction of emitted electrons by the detector. In contrast to the assumption in Fig. 1, the extraction will not be complete in practical cases, allowing an additional current I_R of redistributed electrons to flow. Fig. 2 shows the relevant currents on the surface element, which result in a net charging current of:

$$I_C = -I_P + I_S + I_B - I_R(U_S) \quad (1)$$

I_P, I_S and I_B are assumed to be independent of the surface potential U_S, since the yield curve of most materials has a relatively small slope between the crossover energies. The redistributed current $I_R(U_S)$ increases with positive U_S. The

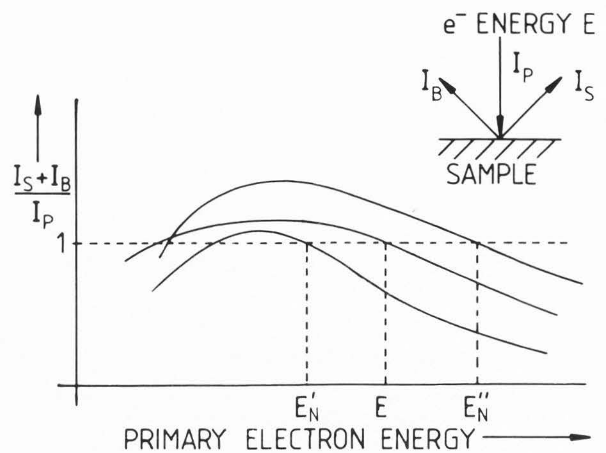

Fig. 1: Schematic yield curves on sample surface areas differing in material composition, roughness or angle (e.g., Gibbons, 1966).

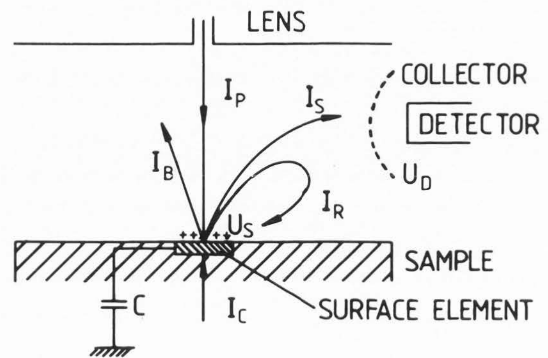

Fig. 2: Currents in the SEM which charge a specimen surface of capacitance C with a resulting current I_C. I_P: primary current, I_B: backscattered current, I_S: secondary current, I_R: redistributed current, I_C: charging current.

secondary electrons are increasingly attracted by the surface as it continues charging. In order to develop a first-order theory yielding an estimate for the time constants in positive sample charging, the increase of I_R with U_S is assumed to be linear. Although the functional dependence will in practice be more complex, this does not totally change the basic behaviour of the effects to be described:

$$I_R = f(U)\, U_S = \frac{1}{\rho} U_S. \quad (2)$$

ρ has the dimensions of resistance and represents the effects of the electric field geometry above the irradiated area. The redistributed current I_R increases until it compensates the emitted currents at a surface voltage of $U_S = U_C \leq U_D$ which

stops further charging by $I_C = 0$:

$$-I_P + I_S + I_B = I_R(U_C). \quad (3)$$

Equations 1 and 3 then yield:

$$I_C = I_R(U_C) - I_R(U_S) \quad (4)$$

The current I_C causes an increase of the surface potential U_S towards U_C, which can be calculated using eq.2 analogously to the case of a capacitor being charged via a resistor:

$$U_S(t_i) = U_C\left(1 - e^{-\frac{t_i}{\rho C}}\right) \quad (5)$$

It should be noted if the surface charges to values accelerating the primary beam to such an extent that it attains almost crossover energy. The approximation of I_S = const is not applicable in this case.

Floating conductor

During the e-beam dwell times t_{i+n} on the next surface elements i+n, the potential continues increasing according to eq.5 as long as part of the continuous conductor is scanned. The conductor may, for example, be the chromium layer of a mask or a metal line of a chip. A change of the potential distribution in the area above the conductor goes hand in hand with the charging as depicted in Fig. 3. This causes the redistributed current I_R to increase until it compensates the emitted currents according to eq. 3, allowing a maximum surface potential U_C to be attained. The actual voltage of a floating conductor on the sample surface depends on its capacitance C to ground, the constant ρ and the total time of exposure to the electron beam during the scan.

Insulating material

The electron beam moves on to the next surface element i = 2 after the first one (i = 1) has been charged to $U_S(t_1)$. Electrons emitted from the new surface element are again extracted by the SEM detector but, depending on the electric fields on the sample surface (Fig. 4), also by the positively charged neighboring element. This gives rise to a current of redistributed electrons of:

$$I_R'(U_S) = \frac{1}{\eta} U_S, \quad (6)$$

discharging the previously charged element i = 1. Again a linear dependence on U_S has been assumed to serve as a first order approach. This assumption neglects the influence of charged neighbouring surface areas on the trajectories of redistributed secondary electrons. The discharging of the element during the frame time T due to this current is given by:

$$U_S = U_S(t_i)\, e^{-\frac{1}{\eta C} T}. \quad (7)$$

The values η and ρ will be of the same order of magnitude, since the redistributed currents I_R and I_R' are both determined by similar electric field distributions above the sample. The time constants $1 / \eta C$ and $1 / \rho C$ will therefore also be similar, resulting in a substantial discharging of the surface element as early as during the scan over the next few adjacent ones.

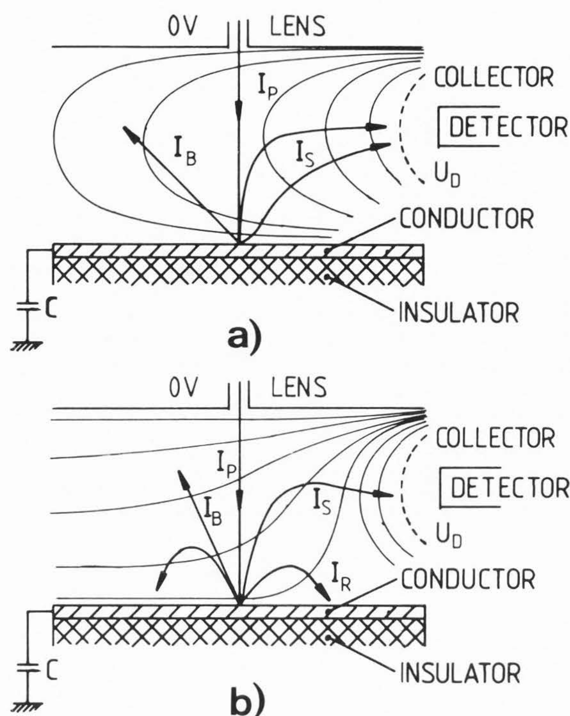

Fig. 3: Potential distribution above a conductor in the SEM chamber before and after positive charging.
a) Electron bombardment just starting, t = 0, $U_S = 0$.
b) Stable potential $U_S = U_C \leqq U_D$ attained, $t = t_C$.

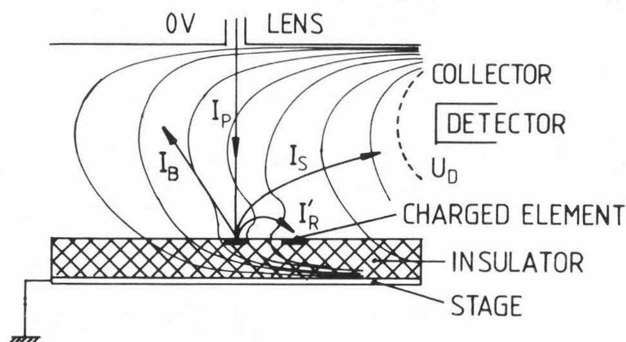

Fig. 4: Potential distribution above an insulator in the SEM chamber after a surface element is charged to a positive voltage. A current I_R'' of redistributed electrons discharges the element while other areas of the surface are scanned.

The total progressive charging and discharging of the scanned surface may be described by a theory considering the capacitance varying with time in a similar way as described by Crawford (1980), but the development of a complete theory is not the subject of the present paper. Nevertheless, the considerations stated demonstrate that positive charging is less on insulators than on conductors.

Influence of charging effects on measurement accuracy

It is well known that negative charging causes deviations in the line width measurement accuracy which have been quantitatively investigated by Frosien and Lischke (1984). These investigations continue to yield additional results on different combinations of materials. The measurement accuracy with beam energies below E_N is studied in more detail with a consideration of positive charging as well.

Several combinations of materials have been investigated. Two examples of quantitative results are shown in Figs. 6 and 7. The line width W and the pitch P (Fig. 5) were measured with different primary energies in a Hitachi S 800 field emission SEM. Measurements were done on the photographs recorded. Calibration values W_{cal} and P_{cal} were obtained on the samples after coating with gold by reproducing the same sequence of primary energies. The relative line width error is calculated by:

$$\frac{\Delta W}{W} = \frac{W \dfrac{P_{cal}}{P} - W_{cal}}{W} . \qquad (8)$$

The measured values W were corrected by the factor P_{cal} / P to eliminate systematic deviations e.g. due to the photographic process and drift effects of the instrument. this additionally corrects part of the global charging effects. The remaining local effects cause increasing deviations above a certain threshold energy towards larger or smaller values, depending on which part of the sample starts charging. There are other additional effects occurring together with the beam displacement such as contrast changes in the image. But these do not change the conclusion not to operate under these conditions of negative charging for quantitative measurements.

No effects due to positive charging have been observed in quantitative investigations in which only insulating materials or conductors having contact to ground are involved (e.g., Fig. 6). This is in agreement with the theoretical statement in the preceding section. These measured values below the threshold energy show deviations of about 0.1 µm (5 to 10% on 2 µm structures), which is the current error in evaluating the SEM images. This error may be reduced by improving the instrument, e.g. eliminating line interference at low-voltage SEM operation.

Unlike the results on insulators, pronounced measurement errors occur with chromium structures on glass even in the low primary energy region (Fig. 7). According to the theory, the chromium squares charge to a positive voltage deflecting the primary beam towards the center of the squares, away from the large chromium area surrounding the squares (lower tooth-like structure in Fig. 7a). The resulting image simulates a larger gap between the outer squares and the surrounding chromium. The large error arises only at the outer edges of the positively charged chromium squares which oppose the surrounding chromium area. The large chromium area does not charge noticeably since it has high capacitance to ground and is irradiated only for relatively short periods. A high field gradient is therefore formed between the squares and the adjacent area deflecting the primary beam. Additional effects related to the process of secondary signal formation also cause measurement errors (Nyyssonen and Postek 1985). These effects do not depend on metal structure capacitances and therefore do not cause the same kind of deviations in measuring the gap between squares or between these and the outer structure. The errors observed here are therefore attributed to charging.

Conclusions with respect to resolution, contrast and distortion

Negative charging in e-beam inspection and metrology can be avoided by using primary beam energies below the crossover values of all surface components. Significant measurement inaccuracies due to positive charging have not been observed on insulators with low-voltage operation. Deviations were less than about 0.1 µm, which is the current accuracy of image evaluation. This value just meets present requirements but has to be improved for future applications.

On floating conductors, on the other hand, measurement errors and image distortions were found to be due to positive charging. The different behavior of insulators and conductors with respect to positive e-beam charging stems from the differences in electric field distribution on the respective surfaces.

Acknowledgements

The authors wish to thank N. Lehner, K. Anger, G. Unger and H. Demuschewski for making available the different samples investigated in the low voltage SEM. They also acknowledge stimulating discussions with J. Frosien and B. Lischke.

References

Brunner M, Menzel E. (1983). Surface potential measurements on floating targets with a parallel beam technique. J. Vac. Sci. Technol. B 1, 1344-1347.

Crawford CK. (1980). Ion charge neutralization effects in scanning electron microscopes. Scanning Electron Microscopy 1980; IV: 11-25.

Frosien J. (1986). Digital image processing for micrometrology. J. Vac. Sci. Technol. B 4(1), 261-264.

Frosien J, Lischke B. (1984) Micrometrology with electron probes. Microcircuit Engineering 84, 441-450, eds. A. Heuberger and H. Beneking, Academic Press.

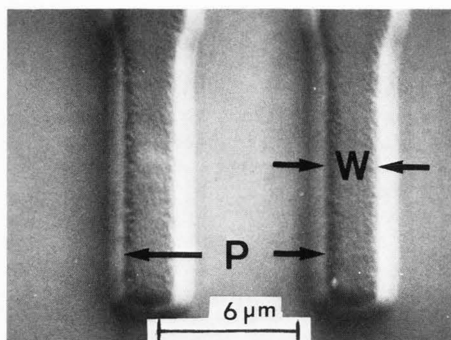

Fig. 5: SEM image of a resist structure on Si_3N_4 recorded by scanning with 800 eV primary electrons. W: line width, P: pitch

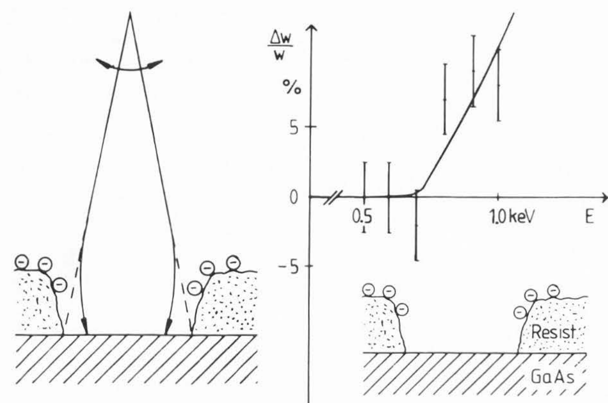

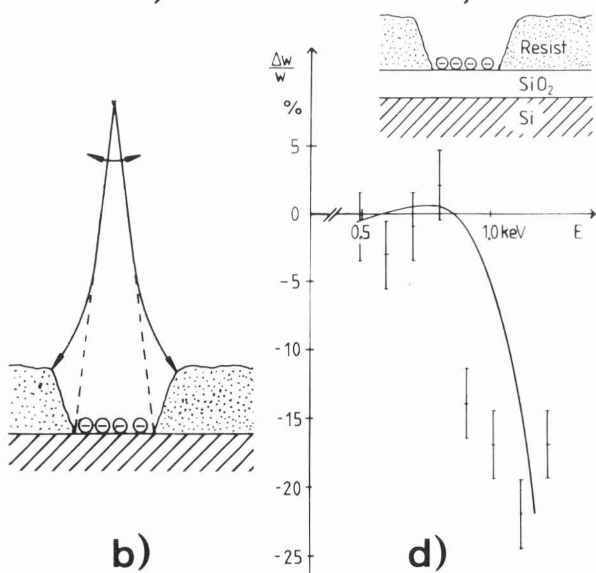

Fig. 6: Deflection of the scanning beam simulating a) a larger line width and b) a smaller line width. c) and d) relative line width measurement errors on resist structures versus primary e-beam energy. The error range of the image evaluation is about ±2.5 % as indicated, depending on the image contrast. The line width measurement error below the threshold energy is in the same range.

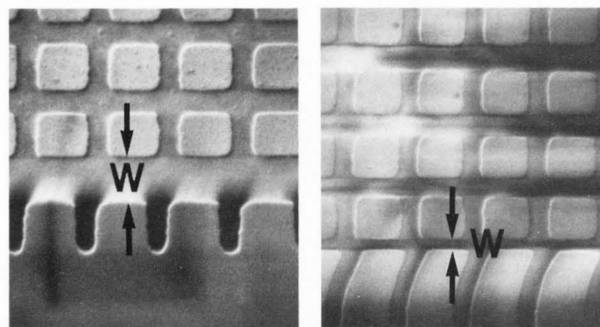

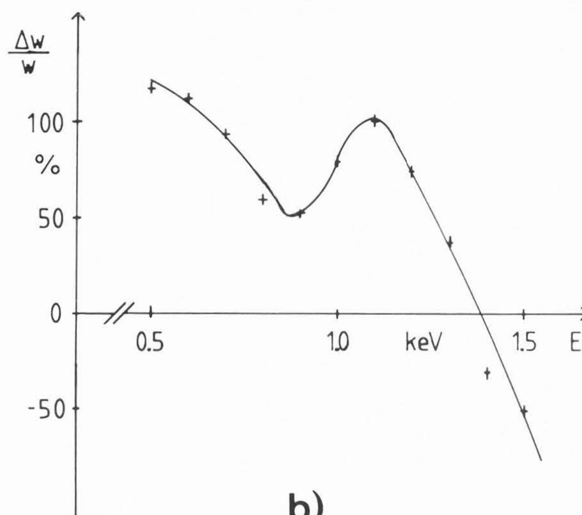

Fig. 7: a) SEM images of chromium squares on glass with 700 eV and 1400 eV primary energy. The gap size W changes with beam energy. b) relative measurement error of the gap size versus primary beam energy.

Gibbons DJ. (1966) Secondary electron emission. Handbook of Vacuum Physics, Vol. 2: Physical Electronics, 301-395, A. H. Beck (ed.), Pergamon Press.

Hembree GG, Jensen SW, Marchiando JF. (1981). Monte Carlo simulation of submicrometer linewidth measurements in the scanning electron microscope. Microbeam Analysis, 123-126, R.H. Geiss (ed.), San Francisco, CA 94105.

Jensen S, Swyt D. (1980). Sub-micrometer length metrology: problems, techniques and solutions. Scanning Electron Microsc. 1980; I: 393-406.

Jensen S, Hembree G, Marchiando J, Swyt D. (1981). Quantitative sub-micrometer linewidth determination using electron microscopy, SPIE*) 275 Semiconductor Microlithography VI, 100-108.

Nyyssonen D, Postek MT. (1985). SEM based system for calibration of linewidth SRMs for the IC industry. SPIE*) 565 Micron and Submicron Integrated Circuit Metrology, 180-186.

Postek MT. (1983). The scanning electron microscope in the semiconductor industry. Test & Measurement World, Sept 1983, 54-72.

Postek MT. (1984a). Low accelerating voltage inspection and linewidth measurement in the scanning electron microscope. Scanning Electron Microsc. 1984; III: 1065-1074.

Postek MT. (1984b). Critical dimension measurement in the scanning electron microscope. SPIE*) 480 Integrated Circuit Metrology II, 109-119.

Russel PE, Namae T, Shimada M, Someya T. (1984). Development of SEM-based dedicated IC metrology system. SPIE*) 480 Integrated Circuit Metrology II, 101-108.

Seiler DG, Sulway DV. (1984). Precision linewidth measurement using a scanning electron microscope. SPIE*) 480 Integrated Circuit Metrology II, 86-93.

Yamaji H, Miyoshi M, Kano M, Okumura K. (1985). High accuracy and automatic measurement of very large scale integrated circuits. Scanning Electron Microsc. 1984; I: 97-102.

Discussion with Reviewers

L. Reimer: Do you think the change in apparent linewidth is caused only by deflection of primary electrons as indicated in Figs. 6a,b? The secondaries are influenced much more by the charging as Fig. 7 shows, for example. Because of the problem, at which point a linewidth measurement has to start, changes in contrast can change this point indicated by the human vision system.

M.T. Postek: You seem to advocate that all of the measurement errors observed on the samples you used are related to only charging effects. I would like to have the author's comments if they feel that other physical mechanisms could play a role in the measurement errors.

Authors: A section has been added to the text to explain why we think the observed effects are due to primary beam displacement caused by charging. To discuss this in more detail: our goal was not to show that charging is the only reason for errors but that it is an additional one which has not been investigated so far. The strong increase of the measurement error with increasing primary energy, which starts at a certain threshold energy, is attributed predominantly to charging because there is no effect of this kind on conducting samples. It is assumed that the effects of contrast changes are minor in our measurements since the evaluation was done visually and much care was taken always to identify the same detail of the edge. This was possible because there is a gradual increase of charging with rising primary energy and the changes in contrast can be followed visually. But, of course, there is an additional strong contrast effect especially with automated measurements when the edge position is determined by a signal threshold. The effect of positive charging is discussed in the preceding text, but it may be added that curved image structures were observed in many cases, which, in our opinion, can only be explained by beam displacement.

K.D. Herrmann: How can the relative minimum in fig. 7b) be explained?

Authors: The sample contains chromium and glass. Both can charge because the chromium is not connected to ground since it is not a continuous structure. Both charge positively at low primary energy. Above a certain energy one of both materials starts charging negatively resulting in a very non-uniform potential distribution. This distribution depends on the individual sample structure. The measurement error on a certain sample area, on the other hand, depends on the specific distribution of the local potentials. In addition, the effects of redistributed currents are also controlled by the local potentials. The minimum in Fig. 7b) is assumed to be due to the energy dependence of these local potentials. We therefore see no way for a general description of beam displacement.

K.D. Herrmann: How does the measurement error depend on the irradiation time for taking the image?

Authors: This has not been investigated in detail but it has been observed that errors decrease with increasing scan frequency - which is also commonly known.

J.B. Pawley: Is it possible to estimate surface potentials by the change in focus current required to produce a sharp image from a particular area of the sample?

Authors: This is probably not possible on practical samples because the complexity of the charged structure on integrated circuits causes a very non-uniform potential distribution. The focus conditions on the area of interest are strongly influenced by the potential attained by adjacent areas. In addition, the astigmatism introduced by the non-uniform potential is much stronger than the defocus.

---

*) SPIE: Society of Photo-Optical Instrumentation Engineers, P.O. Box 10, Bellingham, Washington 98227, USA